Stabilization of ZnO Nanoparticles Using Water Extract of Waste Coconut Husk and Photocatalytic Activity

Sanjib Baglari
Central Institute of Technology Kokrajhar
Dulu Brahma
Central Institute of Technology Kokrajhar
Ujjal K Gautam
IISER Mohali: Indian Institute of Science Education and Research Mohali
Pranjal Kalita
Central Institute of Technology Kokrajhar
Manasi Buzar Baruah (mbbaruah@cit.ac.in)
Central Institute of Technology Kokrajhar https://orcid.org/0000-0002-3820-6069

Research Article

Keywords: Photocatalysis, Coconut husk ash, Methyleneblue, Methyl orange, Rate constant

Posted Date: September 8th, 2021

DOI: https://doi.org/10.21203/rs.3.rs-688693/v1

Stabilization of ZnO Nanoparticles Using Water Extract of Waste Coconut Husk and Photocatalytic Activity

Riu RiuWary[1], Sanjib Baglari[1], Dulu Brahma[2], Ujjal K Gautam[3], Pranjal Kalita[2]
Manasi Buzar Baruah[1,*]

[1]Department of Physics, Central Institute of Technology Kokrajhar (Deemed to be University, MoE, Govt. of India), Kokrajhar-783370, Assam, India
[2]Department of Chemistry, Central Institute of Technology Kokrajhar (Deemed to be University, MoE, Govt. of India), Kokrajhar-783370, Assam, India
[3]Indian Institute of Science Education and Research Mohali, Department of Chemical Sciences, Knowledge City, Sector 81, SAS Nagar, Manauli-140306, India

*Corresponding author
Email: mbbaruah@cit.ac.in

Abstract

Here, we report the synthesis of highly photoactive zinc oxide nanoparticles using water extract of waste coconut husk ash as a precipitating agent in a green approach which is a potential source of natural alkaline media. The formation of zinc oxide nanoparticles at different pH of the solution of coconut husk ash was confirmed through powder XRD, SEM-EDX, UV-Vis, FTIR and photoluminescence spectroscopy. The photocatalytic performance of the samples was evaluated through the degradation of methylene blue (MB)and methyl orange (MO) under solar irradiation which undergoes degradation around 98% and 56% within 120 min, respectively. The high photocatalytic activity and rate constant could be attributed to the large surface area due to small particle size that could provide quicker photon absorption and reduction of charge carrier recombination. This current work introduces a new method to reduce energy consumption for the synthesis of highly photoactive low-cost zinc oxide nanoparticles.

Keywords: Photocatalysis . Coconut husk ash . Methyleneblue . Methyl orange . Rate constant

Introduction

Semiconductor materials have gained significant attention in the scientific community due to their various applications for the past decades (Theerthagiri et al. 2019). There are various kinds of semiconductors such as CeO_2, ZnO, CuO, WO_3, Fe_2O_3 and TiO_2have been studied widely for diverse technical applications. Among them, ZnO has been attracting more attention due to its good optoelectronic properties, inexpensive, stability, catalytic and nontoxic behavior. ZnO is an n-type semiconductor of group II-IV with high optical band gap energy of 3.37 eV and excitation binding energy of 60 meV which ensures efficient emission depending upon the situation set up at room temperature and the materials come into existence in three different structures *viz,* Rocksalt, Zinc blende and Wurtzite (Ong et al. 2018). Wurtzite is the most thermodynamically stable form of zinc oxide at ambient conditions. The materials exist unique optical and electrical properties in their nanoscale order and these are becoming responsible for potential applications in the field of solar cell (Saboor et al. 2019), laser diode (Deng et al. 2020), photocatalysis (Das

et al. 2018), light emitting device (Lu et al. 2017).Zinc Oxide is considered to be one of the attractive semiconductors in the field of photocatalysis for the mineralization of organic dye in water as compared to TiO_2 (Shinde et al. 2017,Li et al. 2009). The high quantum efficiency and the capability to absorb large faction of the solar spectrum are the discernible reasons which lead ZnO to become more novel material for wastewater treatment. The photocatalytic activity of such kind of materials are influenced by their band structure, surface morphology and crystallinity, hence there is a deep correlation among the mentioned parameters (Payra et al. 2020).

Conventionally, alkaline solution is used as a precipitating agent to prepared ZnO NPs, where the reaction between OH^- species and Zn^{2+} ion in the alkaline solution form intermediate species and the formation of ZnO takes place directly. As a source of OH^-, alkaline metal hydroxide, like KOH, NaOH and LiOH have been used as a synthetic base for the production of ZnO NPs (Shamhari et al. 2018, Adam et al. 2018, Radzimska et al. 2018). Moreover, the utilization of such a synthetic base reduces the impurity of the NPs in the final product but its chemical process during the formation of NPs consumes a large amount of energy. Concerning these, synthesis of ZnO NPs through green technology become popular for photocatalytic and antibacterial applications as an alternative technique to reduce energy consumption as well as limit the use of toxic and expensive chemicals. Different parts of plant extract, microorganism and algae have been employed to prepare the ZnO NPs, however the microorganism process is time consuming and demands critical protocol. To resolve all such issues, waste green materials are another alternative to synthesize the ZnO NPs. Recently, Phongarthit et al. synthesized ZnO NPs using water extract of wood ash and observed better photocatalytic activity than ZnO NPs prepared in the presence of an aqueous solution of NaOH as a precipitating agent (Phongarthit et al. 2018).

Coconut husk ash contains a large amount of potassium in the form of chloride or oxide as a major component and has been used as a catalyst for different purposes (Husin et al. 2018, Narayanan et al. 2019). Generally, in North East India (especially in Assam), water extract of waste coconut husk ash has been used as a food additive, soaps, and detergents. The art of state demands that till now no one has reported the use of coconut husk ash water extract as a precipitating agent to synthesize ZnO NPs. The coconut husk ash water extract is found to be high pH value around 13 which indicates that it is highly basic in nature. We believe that it could be replaced commercially available precipitating agent like NaOH and KOH. From the literature review, it is clear that the present study would be the first report using coconut husk ash water extract as a precipitating agent for the preparation and characterization of ZnO NPs. The prepared ZnO NPs catalyst was investigated for photocatalytic activity through the degradation of methylene blue and methylene orange under solar irradiation.

Materials and methods

Materials

Coconut was obtained from Blagaon market, Kokrajhar, Assam, India. Zinc nitrate hexahydrate [$Zn(NO_3)_2.6H_2O$]. Methylene blue and methyl orange were obtained from Merck (India) and used without any further purification.

Preparation of coconut husk ash water extracts (CHAWE)

In order to obtain coconut husk ash (CHA), coconut husk was cut into small pieces, washed with de-ionized water and then air dried for 15 days. Further, it was kept in oven for completely dry. Then, dried coconut husk was burnt to ashes and the final product was ground in a mortar pestle.

Afterward, three different stock solutions were prepared by adding different amounts of CHA in each 100ml deionized water to obtain the different ranges of pH. Each mixture was stirred for 30 min and filtered using whatman No. 1 filter paper and placed in normal temperature for further use.

Synthesis of ZnO NPs

For our study, we have synthesized ZnO NPs by co-precipitation method. From each stock solution 60 ml of CHAWE was taken in a beaker and placed on magnetic stirrer at constant 900 rpm. To the mixture, 0.2M aqueous solution of [$Zn(NO_3)_2$] was added on each beaker and observed white milky mixture after a few minutes that was left for 2 h under constant stirring at normal temperature. Afterward, white milky precipitate was collected and washed with distilled water. Then, finally washed with ethanol for many times to eliminate impurities and products were dried in an oven at 50^0C for overnight. To obtain the desired materials, the products were grinded into powder and calcined at 400^0C for 1 h, later on, it was kept in desiccators for further characterizations. The prepared three samples are referred as ZnO NPs-pH 8.6, ZnO NPs-pH 10.4 and ZnO NPs-pH 12.7.

Characterization

The crystallinity and pure phase formation of the prepared samples were identified by powder X-Ray diffraction (PXRD) using PANalytical X'PERT, Netherlands with CuKα as an incident beam (λ=1.54 Å) and patterns were recorded in the ranges of 20-$80^0$with a scanning rate of 1°/min. Functional group in the material was recorded by FTIR technique in the frequency ranges between 400-4000 $cm^{-1}$with resolution of 0.5 cm^{-1}using KBr pellet on Shimadzu FTIR 8201. Optical properties of the prepared materials were studied using diffuse reflectance spectra (DRS) at normal temperature in the wavelength range of 250-800 nm on UV-Vis DRS spectrophotometer using Shimadzu UV-2600. Surface morphology and elemental composition of synthesized ZnO NPs were examined using scanning electron microscopy (SEM, JSM-7600F), and energy dispersive X-ray spectroscopy (EDX) using model Oxford Instruments. Photoluminescence (PL) was carried out using spectrophotometer (PL, Horiba Scientific).

Photocatalytic activity

To know the catalytic activity of the prepared ZnO NPs catalysts, we have performed photocatalytic activity by the degradation of methylene blue (MB) and methyl orange (MO) under natural solar irradiation. In the typical procedure, 0.5g/l catalyst was loaded into 0.01mM MB solution. After that catalyst was loaded into MB solution and then placed in dark for 30 minutes before exposing them into solar irradiation to attain adsorption-desorption equilibrium. To know the progress of degradation of methylene blue, 2 ml solution was collected after every 20 minutes from a magnetically stirrer and further centrifuged to eliminate the catalyst. The degradation efficiency of the sample was monitored by observing maximum absorption spectra of MB and MO against time at a wavelength of 663 and 464 nm respectively using a UV-Visible spectrophotometer.

The catalytic degradation efficiency (%) was evaluated using the following relation-

$$\text{Degradation efficiency (\%)} = \frac{C_0 - C}{C_0} \times 100\ \% = \frac{A_0 - A}{A_0} \times 100\ \%$$

WhereC_0 indicates initial concentration of catalyst loaded MB solution and C is the final concentration of the aforementioned solution after solar irradiation at different time. A_0 and A are the absorbance of the samples before and after the catalytic reaction.

Result and discussion

ZnO NPs formation mechanism from ash-alkali extract

Potassium (K) and Sodium (Na) are members of the group I of periodic tables which are bound in the organic matrix of plants may form carbonates and hydroxide ion in water and water soluble alkali oxides such as K_2O and Na_2O.

$$K_2CO_3(aq.) \rightarrow 2K^+(aq.) + CO_3^{2-}(aq.) \quad (1)$$

$$K_2O\,(aq.) \rightarrow 2K^+(aq.) + OH^-(aq.) \quad (2)$$

$$H_2O\,(l) + CO_3^{2-}(aq.) \rightarrow HCO_3^{2-}(aq.) + OH^-(aq) \quad (3)$$

$$H_2O\,(l) \rightarrow H^+(aq.) + OH^-(aq) \quad (4)$$

$$H^+(aq.) + CO_3^{2-}(aq.) \rightarrow HCO_3^-(aq.) \quad (5)$$

The increasing pH value of the solution with the addition of CHA may be due to the abstraction of H^+ion by CO_3^{2-} from the water which increases OH^- ion in the solution according to the above Eq. 1-5. The following probable reactions are believed to involve during the formation of ZnO NPs at different pH values.

$$Zn(NO_3)_2.6H_2O \rightarrow Zn^{2+}\ 3NO_3^- + 6H_2O \quad (6)$$

$$Zn^{2+} + 2OH^- \rightarrow Zn(OH)_2 \quad (7)$$

$$Zn(OH)_2 + 2OH^- \rightarrow [Zn(OH)_4]^{2-} \quad (8)$$

$$[Zn(OH)_4]^{2-} \rightarrow ZnO + H_2O + 2OH^- \quad (9)$$

Powder XRD and structural study

The powder X-ray diffraction (PXRD)pattern of the ZnO NPs prepared at different concentrations with pH is shown in Fig. 1. All the diffraction peaks corresponding to different crystal planes are in good agreement with JCPDS card no. 89-0510 which confirms the hexagonal wurtzite phase formation of the ZnO NPs. The high intensityof diffraction peaks signifies a good crystal quality of ZnO NPs. Also, the intensity of diffraction planes reveals the oriented growth of structure. The higher intensity of (101) diffraction plane of observed XRD spectra of samples represents the oriented growth along (101) direction (Kumari et al. 2010). Furthermore, the broad diffraction peak gives an idea of small crystallite size. No other additional peaks were detected in addition to it, with increasing basicity, the intensity of (101) peak diminishes, signifying degradation of crystallinity of the nanoparticles

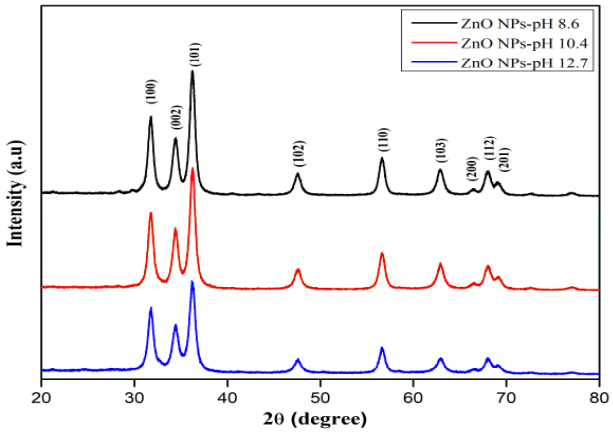

Fig. 1 XRD spectra of ZnO NPs prepared at different pH value.

The crystallite size (D) and lattice strain (Ɛ) are calculated from Williamson-Hall (W-H) method (Supplementary information "S1") and the values are shown in Table 1. The specific surface areas of the samples were calculated using the equation S = 6000/ρ D, where ρ is the materials density and D is the crystallite size. The lattice parameters (a and c) and cell volume (V) of the prepared ZnO NPs with hexagonal wurtzite phase were calculated from the following relation

$$\frac{1}{d_{hkl}^2} = \frac{4}{3}\left\{\frac{h^2+hk+k^2}{a^2}\right\} + \frac{l^2}{c^2} \qquad (10)$$

$$V = 0.866 \times a^2 \times c \qquad (11)$$

Where d_{hkl} is the inter-planar spacing of plane (hkl).

W-H is the modified straight line equation which is known as Uniform Deformation Model (UDM), where the uniform assumption was taken in all crystallographic directions. W-H plot shows the negative strain of all samples representing compressive strain. The increase in lattice strain has been observed with decreasing crystallite size of the samples and it is shown in Table 1. This is because of small crystallite size and more surface atoms in the materials which generate a stress field in the grain boundaries. This generated stress field in the materials induces the lattice distortion which may be the reason of increasing strain value from 1.36 to 2.70 with decreasing crystallite size. In addition to it, the reduction in the volume of the unit cell can be attributed to the increase of surface stress with reducing crystallite size from pH 8.6 to 12.7. Interestingly, we observed that the crystallite size decreases from 9.05 to 8.15 nm. The lattice parameter calculated from (002) and (101) crystalline planes using Eq. 10 was found to be very close to the standard JCPDS card no. 89-0510.

Table 1 Crystallite size and lattice parameters of ZnO NPs

Sample	**W-H plot**		**Lattice parameters**				
	Average Crystallite Size (nm)	Surface Area(m^2/gm)	Strain (10^{-3})	a=b (Å)	c (Å)	c/a ratio	V (Å^3)
ZnO NPs-pH 8.6	9.09	117.67	1.36	3.251	5.203	1.600	47.640
ZnO NPs-pH10.4	8.92	119.90	1.71	3.249	5.208	1.602	47.625
ZnO NPs-pH 12.7	8.15	131.23	2.70	3.249	5.202	1.600	47.568

Elemental and scanning electron microscopy (SEM) study

The chemical constituent present in the prepared materials has been investigated using energy dispersive X-ray spectroscopy (EDX). The EDX spectra of all the prepared samples show the constituents of Zn and O and overall, all of the samples possess almost similar chemical compositions (Supplementary information Fig. S2). This result indicates that no other impurity atom has been observed and the existence of a single phase in the desired product that also confirmed by XRD analysis. It is also noticed that the weight and atomic percentage of Zn in the materials are increased with increasing the pH and it is shown in Fig. S2. The SEM micrographs of all the prepared samples are shown in the Fig 2. It is observed that the ZnO NPs possess relatively small particles of average size 9-14 nm. When a chemical reaction occurs between ZnO and excess OH^- ions, the dissolution occurs (Daneshvar et al. 2007), which made the crystallite size smaller and agglomerated. The reduced crystallite size with a variation of pH has been also reported by other literature (Alias et al. 2010, Kumaresan et al. 2017). The observed average size of the particles is in good agreement with the size observed using W-H plot from XRD analysis.

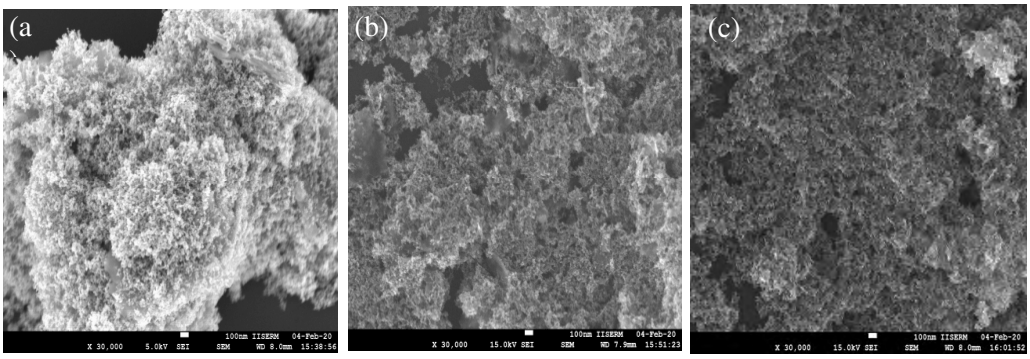

Fig. 2 Scanning electron microscope (SEM) micrograph at (a) pH 8.6 (b) pH 10.4 & (c) pH 12.7 using coconut husk as a natural alkaline solution

UV-Vis Spectroscopy

The study of diffuse reflectance spectroscopy was carried to analyze the optical properties of the samples and shown in Fig. 3 (a). F(R) derived from $F(R) = \frac{(1-R)^2}{2R}$is equivalent to the absorption coefficient where R represents the reflectance of the particles. All the samples have been found to be strong absorber in the UV region i.e. below 400 nm, this could be attributed to the absorption of a large fraction of photon energy by electrons in lower energy quantum state in different energy levels of the valance band. The optical band gap energy of the NPs is determined by plotting Tauc's graph [Fig. 3(b)]. The estimated optical band gap energies are 3.29, 3.28 and 3.24 eV corresponding to the sample ZnO NPs-pH 8.6, 10.4 & 12.7, respectively. Those values are lower than that of bulk band gap energy of ZnO (3.37 eV). It is clearly observed that absorption edges of the samples are slightly red shifted with decreasing crystallite size which indicates the size dependency ability of the particles to absorb UV light. Also, the increase in lattice strain may be responsible for red shift of the observed spectrum which can change the band energy of ZnO NPs. When the size of nanocrystallite is less than that of the exciton Bohr radius, then the quantum confinement effect on the electronic energy gap of semiconductor becomes more prominent where valance and conduction bands are modified by confined charge carries. Also, the Coulomb interaction between hole and electrons has an important role in nanosized solid materials. Alias et al. reported the changes of band gap energy from 3.25 to 3.14 eV with a

decrease in crystallite with an increasing pH value of the solution (Alias et al. 2010) and the result is matched with our present work.

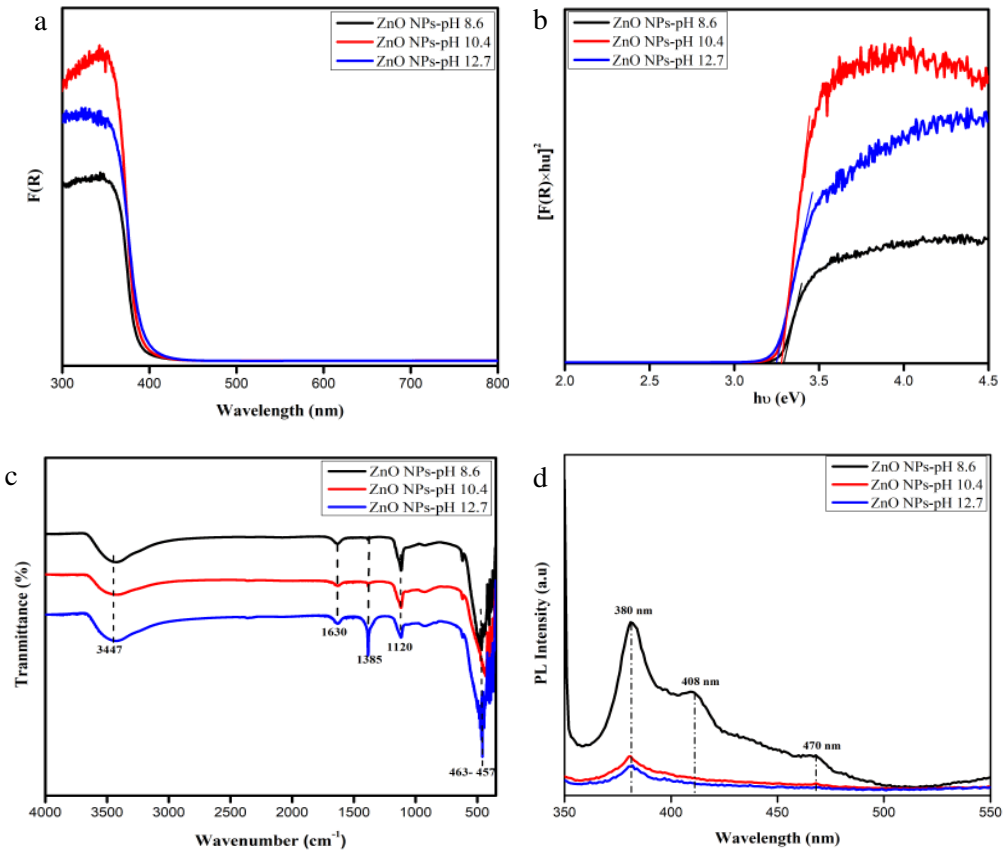

Fig. 3 (a) UV-Vis DRS spectra.(b) Tauc's plot of the sample (c) FTIR spectra (d) PL spectra of ZnO NPs prepared at different pH value.

Fourier-transform infrared spectroscopy

The atomic vibrational mode of synthesized ZnO NPs has been analyzed with the help of FTIR spectroscopy and the spectra are shown in Fig. 3(c). The band at 1630 cm^{1}represents bending vibration of O-H-O mode corresponds to the adsorption of water molecules over the surface of the prepared materials. The transmission peak appeared at 1385 cm^{-1} is due to the presence of impurity of NO_3^- ion left even after washing several times with DI water and ethanol. The peak observed around 1120 cm^{-1} represents the bending mode of Zn-OH. The sharp characteristic bands observed at 463-457cm^{-1} are due to the stretching vibration of Zn-O, which confirms the formation of ZnO NPs. Moreover, all the samples have broadband at 3447 cm^{-1}attributed to the stretching vibration of the O-H group which may be converted to hydroxyl radical by donating an electron to the photogenerated holes (Das et al. 2020). Thus, it is expected that photocatalytic efficiency can be boosted in the presence of such functional group.

Photoluminescence

Photoluminescence (PL) spectroscopy has been carried out to investigate the defects present in the prepared ZnO NPs and the observed spectra are shown in Fig. 3(d). PL spectra of ZnO consist of two luminescent bands i.e. UV-emission (< 400 nm) ascribed to the recombination of photo generated electron with hole, referred as a near band edge

emission (Das et al. 2020) and visible emission band in the range of 400-700nm, associated with various defect states such as interstitials, vacancy, and anti–site of O and Zn, named as deep level emission. It is observed that all the samples exhibit a sharp peak at 380 nm. Moreover, the materials prepared at lower pH has another two distinct peaks at 408 and 470 nm, in which wavelength at 408 nm named as violet emission is associated with electron relaxation process from conduction band tail to the valance band tail states (Kalita et. al 2017) and blue emission and at 470 nm is due to the electron transition from donor level to acceptor level of Zn vacancy (Wei et al. 2007). Interestingly, the intensity of the signature of the excitonic band is found to be decreased for the samples prepared at a higher pH value which indicates the absence of defect site. The lower intensity in the photoluminescence spectra represents decrease in recombination of electron and hole. We believe that, the presence of defect state which provides electron-hole trapping center contributes important role to obtain high yield for photocatalytic efficiency.

Catalytic activity

The photocatalytic activity of synthesized ZnO NPs catalyst was evaluated under solar irradiation using MB as a probe pollutant. As expected from the study of photoluminescence spectroscopy, it is observed from Fig. 4(a) that all the samples prepared at different pH exhibited excellent photocatalytic activity with efficiency of 97.7%, 97.5% and 97.1% (ZnO NPs-pH 8.6, ZnO NPs-pH 10.4, ZnO NPs-pH 12.7) for 120 min respectively, under the same reaction condition. The rate constant was evaluated from the first order plot $-\log(C/C_0)$ vs. time [Fig. 4(c)] and the observed values are 0.0323 and 0.0287 min^{-1} corresponding to ZnO prepared at pH 8.6, 10.4 &12.7 respectively (Das et al. 2020). The photocatalytic activity was also performed for degradation of stable organic pollutant dye such as MO under the similar reaction condition. It is observed that maximum MO degradation is 56% for 120 min with a rate constant value 0.0047 min^{-1}[Fig. 4(b, d)]. The reduction of charge carrier recombination is due to the presence of defect states which contributes in trapping photo generated electrons and the small particle size which provides large surface area for rapid absorption and degradation of MB molecules, contributes to excellent photocatalytic activity of the prepared materials. We have compared our catalytic activity result with ZnO NPs prepared using a different precipitating agent such as leaves extract, peel extract, aqueous NH_3, NaOH and commercially available ZnO and the list is given in Table S1. It is noticed that most of the reaction needs prolong reaction time of 180-270 mins. It reveals that ZnO NPs could be synthesized using natural alkaline media at low cost without the use of any other expensive chemicals which show excellent catalytic activities in less reaction time of 120 mins. Finally, we could suggest that single phase ZnO NPs could be successfully synthesized using coconut husk ash water extract as a precipitating agent in a green approach without the use of any toxic or reducing agents that have excellent photocatalytic activity.

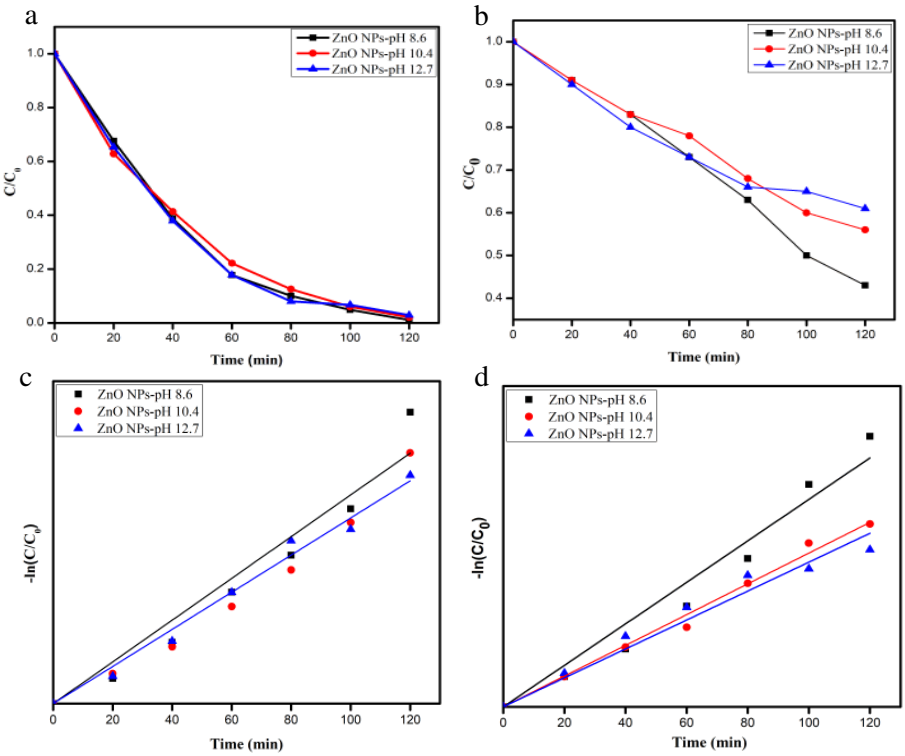

Fig. 4 Degradation and rate constant spectra of MB (a,c) &MO (b,d) under solar irradiation.

Conclusion

In the present work, we have successfully prepared single phase ZnO NPs using an alkaline solution of coconut husk ash water extract as a precipitating agent by co-precipitation method. The photocatalytic activity of prepared samples exhibited excellent degradation of methylene blue under solar irradiation which can be attributed to the large surface area due to the very small particle size and the quenching of charge carrier recombination. Finally, we can conclude that coconut husk ash water extract could be utilized as a precipitating agent which can replace commercially available precipitating agent for synthesis of highly efficient ZnO NPs without using any toxic compound.

Acknowledgement

The authors are grateful to Director, CIT Kokrajhar for his constant support and encouragement.

Authors' contributions Riu Riu Wary designed the methodology, experiment, analysis, writing original draft. Sanjib Baglari and Dulu Brahma collected the resources and helped in data analysis, Ujjal K Gautam characterized the UV-Vis and PL, Pranjal Kalita and Manasi Buzar Baruah supervised the work, reviewed and finalized the manuscript.

Funding There is no fund.

Data availability The data are available upon request.

Compliance with ethical standards

Competing interest The authors declare that they have no competing interest.

Ethical approval For this type of study, formal consent is not required.

Consent to participate The authors agree to participate.

Consent to publish The authors agree to publish.

References

Adam RE, Pozina G, Willander M, Nur O (2018) Synthesis of ZnO nanoparticles by co-precipitation method for solar driven photodegradation of congo red dye at different pH. Photonics and Nanostructures-Fundamentals and Applications 32: 11-18. https://doi.org/10.1016/j.photonics.2018.08.005

Alias SS, Ismail AB, Mohamad AA(2010) Effect of pH on ZnO nanoparticle properties synthesized by sol-gel centrifugation. Journal of Alloys and Compounds 499:231-237. https://doi.org/10.1016/j.jallcom.2010.03.174

Daneshvar N, Aber S, Dorraji MSS, Khataee AR, Rasoulifard MH (2007) Photocatalytic degradation of the insecticide diazinon in the presence of prepared nanocrystalline ZnO powders under irradiation of UV-C light. Separation and Purification Technology 58:91-98. https://doi.org/10.1016/j.seppur.2007.07.016

Das A, Malakar P, Nair RG (2018) Engineering of ZnO nanostructures for efficient solar photocatalysis. Materials Letters 219:76-80. https://doi.org/10.1016/j.matlet.2018.02.057

Das A, Patra M, Bhagavathiachari M, Nair RG (2020) Defect induced visible light driven photocatalytic and photoelectrochemical performance of ZnO-CeO_2nanohaterojunctions. Journal of Alloys and Compounds 858:157730. https://doi.org/10.1016/j.jallcom.2020.157730

Das A, Wary RR, Nair RG (2020) Cu modified ZnO nanoflakes: An efficient visible light-driven photocatalyst and a promising photoanode for dye sensitized solar cell (DSSC). Solid State Science 104:106290. https://doi.org/10.1016/j.solidstatesciences.2020.106290

Das A, Wary RR, Nair RG (2020) Mn-doped ZnO: Role of morphological evolution on enhanced photocatalytic performance. Energy Report 6:737- 741. https://doi.org/10.1016/j.egyr.2019.11.148

Deng G, Zhang Y, Yu Y, Han X, Wang Y, Shi Z, Dong X, Zhang B, Du G and Liu Y(2020) High-Performance Ultraviolet light-emitting diode using n-ZnO/p-hBN/p-Gan contact haterojunctions, ACS Applied Materials & Interfaces 12(5):6788-6792. https://doi.org/10.1021/acsami.9b21894

Husin H, Abubakar A, Ramadhani S, Sijabat CF Br and Hasfita F (2018) Coconut husk ash as heterogeneous catalyst for biodiesel production from cerberamanghas seed oil. MATEC web of Conference 197: 09008. https://doi.org/10.1051/matecconf/201819709008

Kalita A, Kalita M P C (2017) Williamson-Hall analysis and optical properties of small sized ZnO nanocrystals. Physics E 92: 36-40. https://doi.org/10.1016/j.physe.2017.05.006

Kumaresan N, Ramamurthi K, Babu RR, Sethuraman K, S.M. Babu (2017) Hydrothermally grown ZnO nanoparticles for effective photocatalytic activity. Applied Surface Science 418:138-146. https://doi.org/10.1016/j.apsusc.2016.12.231

Kumari L, Li WZ(2010) Synthesis, structural and optical properties of zinc oxide hexagonal microprisms. Crystal Research & Technology 45:311-315. https://doi.org/10.1002/crat.200900600

Li Y, Xie W, Hu X, Shen G, Zhou X, Ziang Y, Zhao X and Fang P (2009) Comparison of dye photodegradation and its coupling with light-to-electricity conversion over TiO_2 and ZnO. Langmuir 26(1):591-597. https://doi.org/10.1021/la902117c

Lu YJ, Shi JF, Shan C X and Shen DZ (2017) ZnO-based deep ultraviolet light-emitting devices. Chinese Physics B 26:047703. https://doi.org/10.1088/1674-1056/26/4/047703

Narayanan DP, Balasubramanyan S, Cherikkallinmel SK, Vadery V, Sankaran S and Narayanan BN(2019) A green approach for the synthesis of coconut husk ash twisted graphene nanocomposites: Novelcatalyst for solvent–free biginelli reaction. Chemistry Select 4: 4785-4796. https://doi.org/10.1002/slct.201803352

Ong CB, Ng LY, Mohammad AW (2018) A review of ZnO nanoparticles as solar photocatalysts: Synthesis, mechanism and applications. Renewable and Sustainable Energy Reviews 81:536-551. https://doi.org/10.1016/j.rser.2017.08.020

Payra S, Ganeshan SK, Challagulla S, Roy S (2020) A correlation story of synthesis of ZnO and their influence on photocatalysis. Advanced Powder Technology 31: 510-520. https://doi.org/10.1016/j.apt.2019.11.006

Phongarthit K, Amornpitoksuk P and Suwanboon S (2018) Synthesis, characterization and photocatalytic properties of ZnO nanoparticles prepared by a precipitation-calcination method using a natural alkaline solution. Materials Research Express 6: 045501. https://doi.org/10.1088/2053-1591/aaf8db

Radzimska AK, and Jesionowski T (2014) Zinc Oxide-From synthetic to application: A review. Materials 7: 2883-2881. https://doi.org/10.3390/ma7042833

Saboor A, Shah SM, Hussain H (2019) Band gap tunig and application of ZnO nanorods in hybrid solar cell: Ag-doped verses Nd-doped ZnO nanorods. Materials Science in Semiconductor Processing 93:215-225. https://doi.org/10.1016/j.mssp.2019.01.009

Shamhari NM, Wee BS, Chi SF, and Kok KY (2018) Synthesis and characterization of zinc oxide nanoparticles with small particle size distribution. Acta Chimica Slovenica 65: 578-585. http://dx.doi.org/10.17344/acsi.2018.4213

Shinde DR, Tambade PS, Chaskar MG and Gandev KM(2017) Photocatalytic degradation of dyes in water by analytical reagent grades ZnO, TiO_2 and SnO_2: A comparative study. Drinking Water Engineering Science 10:109-117. https://doi.org/10.5194/dwes-10-109-2017

Theerthagiri J, Salla S, Senthil RA, Nithyadharseni P, Madankumar A, Arunachalam P, Maiyalagan T and Kim HS (2019) A review on ZnO nanostructured materials: energy, environment and biological applications. Nanotechnology 30:392001. https://doi.org/10.1088/1361-6528/ab268a

Wei XQ, Man BY, Liu M, Xue CS, Zhuang HZ, Yang C (2007) Blue luminescent centers and microstructural evaluation by XPS and Raman in ZnO thin films annealed in vacuum, N_2 and O_2. Physics B 388:145-152. https://doi.org/10.1016/j.physb.2006.05.346

Supplementary Files

This is a list of supplementary files associated with this preprint. Click to download.

- supportinginformation.docx